Supplemental Figure 1 (related to Figure 1). Glucose expands *runx1*+ HSCs in a dose-and duration-dependent manner independent of vascular niche formation.

(A) Increasing concentrations of glucose (0.5%, 1%, 5%) in the fish water exerted a dose-dependent enhancement in *runx1/cmyb* expression by *in situ* hybridization in zebrafish embryos at 36hpf (n≥45/tx).

(B) Duration (12 vs 24hrs) of glucose treatment (1%) (upper panels), but not timing during the onset of hematopoietic development from 12-36hpf, impacted the degree of enhancement in *runx1/cmyb* expression (n≥45/tx). Vascular development (lower panels), assessed by *fli/flk1 in situ* hybridization remained grossly unchanged during all treatment windows (n≥100/tx).

(C) *In vivo* imaging of *fli:GFP* transgenic embryos confirmed normal development of the hematopoietic vascular niche after exposure to 1% glucose from 12-36hpf (n≥35/tx).

(D) qPCR quantification of vascular gene expression (*flk1*, *tie2*, *lmo2*, *ve-cadherin*) revealed significant changes in response to elevated glucose levels in genes highly expressed by both HSCs and endothelium (t-test, *$p<0.005$, n=3).

(E) Exposure to glucose from 12-36hpf rescued *runx1/cmyb* expression in *silent heart* ($sih^{-/-}$) mutant embryos (n≥40/tx).

(F) Morpholino (MO) knockdown of *troponin T type 2,* the gene causing the *silent heart* phenotype, confirmed that reductions in *runx1, cmyb,* and *CD41* expression were rescued by glucose exposure (ANOVA, $p<0.05$, n=3).

Supplemental Figure 2 (related to Figure 1). Glucose specifically enhances cell proliferation in the AGM.

Zebrafish embryos were exposed to 1% D-glucose from 12-36hpf.

(A) Cell proliferation, assessed by whole-mount BrdU staining, was enhanced in response to glucose exposure (22↑/31).

(B) Exposure of *in vivo* proliferation reporter transgenic zebrafish embryos Tg(EF1:mKO2-zCdt1(1/190))rw0405b; Tg(EF1:mAG-zGem(1/100))rw0410h revealed increased cells in S/G2/M phase (green) in the AGM region (n≥50/tx).

(C) Glucose exposure caused a significant increase in the number of BrdU-positive cells in the trunk/tail region encompassing the AGM (t-test, *p<0.001, n=3).

(D) FACS quantification of cell cycle distribution after propidium iodide incubation confirmed a significant increase in cells in G2 after glucose exposure compared to controls (t-test, *p=0.014, n=20).

(E) Hemocytometer counts of whole embryo disaggregates at 36hpf demonstrated no significant change in total cell number after glucose exposure from 12-36hpf (n=6 x3 replicates, t-test, p=NS, n=6 x3 replicates).

(F) Total protein analysis of disaggregrated embryos at 36hpf showed no significant differences after exposure to 1% glucose from 12-36hpf compared to controls (t-test, p=NS, n=3).

(G) Evaluation of the impact of glucose on other mesodermal cell types and germ layers by *in situ* hybridization at 36hpf for *MHC* (muscle), *pax2* (kidney), *cmlc* (heart), *foxA3* (primitive endoderm), and *huc* (Hu antigen C, nervous system) did not reveal any gross morphological changes, confirming the specificity of the effects on the hematopoietic system at this developmental stage (n≥25/tx).

Supplemental Figure 3 (related to Figure 2). Glucose enhances definitive HSC formation and function.

(A) qPCR analysis for HSC-relevant genes *runx1, cmyb,* and *CD41* revealed accelerated and increased induction compared to controls in response to glucose exposure during the onset of definitive hematopoietic development from 18-36hpf (t-test vs 18hpf, $p<0.05$, n=3).

(B) Loss of runx1 in *runx1*$^{-/-}$ mutant zebrafish caused severe impairment of *cmyb* expression by *in situ* hybridization at 36hpf, which could not be rescued by glucose, suggesting *runx1* is required to mediate the effect of glucose on HSCs ($n\geq15$/tx).

(C) Confirmation and quantitation by qPCR analysis of *runx1*-morphants showed the glucose-induced increase in *cmyb* expression is dependent on runx1 (ANOVA, $p<0.05$, n=3).

(D) Detection of donor *CD41:eGFP* cells by microscopy at 3 weeks after transplantation into irradiated adult WT recipients revealed increased fluorescence in recipient fish of AGM cells from glucose-treated embryos (three representative GFP+ samples shown/tx).

(E) FACS analysis of whole kidney marrow (KM) and peripheral blood (PB) in recipients of AGM cells from *CD41:eGFP* embryos at 3 weeks after transplantation revealed increased engraftment rates (GFP+ cells >0.01%; Fisher's exact test, *$p<0.05$).

(F) Replicate experiments confirmed the enhanced engraftment of CD41:eGFP cells in recipients of glucose-exposed AGM cells at 3 weeks post transplantation, as determined by fluorescence microscopy for CD41:eGFP (Fisher's exact (one-tailed), *$p<0.05$, **$p<0.002$, $n\geq10$/tx).

(G) PB FACS analysis for CD45:dsRed in CD41+ engrafted recipients of control and

glucose-treated AGM cells from *CD41:eGFP; CD45:dsRed* donor embryos shows equal potential for multilineage engraftment (FSC/SSC).

Supplemental Figure 4 (related to Figure 2). Glucose exposure enhances hematopoiesis throughout development

(A-C) Embryos were exposed to glucose from 12-24hpf, and effects on primitive hematopoiesis were assessed (n≥35/tx).

(A,B) Glucose exposure increased cell number in transgenic reporters for primitive hematopoiesis, *scl:eGFP*, *gata1:dsred*, and *globin:eGFP* at 24hpf as shown by fluorescence microscopy and (B) FACS (t-test, scl, gata1: *p<0.001, globin: **p<0.05, n=3-9).

(C) qPCR quantification in 36hpf embryos confirmed significantly enhanced gene expression following glucose exposure (t-test, scl, globin: *p<0.001; gata1: **p=0.02, n=3).

(D) Glucose exposure for 24 hrs from 12-36hpf increased *CD41*+ cells in the CHT at 72 hpf or the kidney at 144 hpf in *CD41:eGFP* transgenic zebrafish by determined by fluorescence microscopy (n≥35/tx).

(E) FACS quantification of CD41:eGFP+ cells (from embryos in D) confirmed the sustained elevation of HSCs after glucose exposure up to 144 hpf (t-test, *p<0.05, n=6).

(F) qPCR for the expression of lineage-specific genes (*lysc, mpo, rag2, lck*) confirmed the lack of significant impact on lineage differentiation after glucose exposure from 12-36hpf (t-test, p=NS, n=3).

(G) FACS analysis of lineage-specific reporter embryos (*lysc:dsRed, mpo:GFP,*

rag2:GFP) at 72 and 144 hpf revealed no significant changes in % distribution between untreated and embryos exposed to glucose from 12-36hpf (t-test, p=NS, n=8).

(H) Whole embryo cell counts indicated a significant and persistent increase in total embryo cell number during development after initial glucose exposure from 12-36hpf (t-test, 72 hpf: 30,366±777 vs 34,200±600, p=0.02, n=3; 144 hpf: 43,066±1358 vs 46,700±1735, p=0.046, n=3).

(I) Calculations of absolute numbers of differentiated myeloid cells demonstrate glucose exposure significantly increases total hematopoietic cells at 72 and 144 following exposure from 12-36hpf (t-test, *p<0.05, n=3).

(J) Kidney marrow FACS analysis of zebrafish exposed to glucose from 12-36hpf and analyzed at 1 month post treatment revealed no alterations in lineage distributions and reestablishment of normal HSC number (t-test, p=NS, n=9).

(K) FACS analysis of *CD41:eGFP* embryos at 72 and 144hpf revealed continued susceptibility to the effects of transient (24hr) glucose exposure even at larval stages (t-test, *p<0.05, n=10).

(L) Glucose exposure significantly increased the percentage of hematopoietic precursors in kidney marrow, as assessed by FACS, at day 10 post irradiation injury of adult zebrafish (t-test, *p<0.001, n=10).

Supplemental Figure 5 (related to Figure 5). Reactive oxygen species, but not insulin, play a major role in HSC formation during development.

(A) Prior to pancreas formation and function at 36hpf, treatment with the beta-cell toxin streptozocin had no effect on *insulin* expression in control or glucose-exposed embryos

(n≥40/tx).

(B) Exposure to oxidants PTU (0.003%), BSO (500μM), and paraquat (500μM) from 10-36 hpf enhanced *runx1/cmyb* expression at 36 hpf (n≥40/tx).

(C) Antioxidants and ROS inhibitors vitamin C (750μM), Euk134 (500μM), and MitoQ (10μM) decreased *runx1/cmyb* expression and blocked the effects of glucose (n≥30/tx).

(D) Use of an intravital H_2O_2 sensor (green), Peroxy-Fluor 2 (PF2), in *lmo2:dsRed* transgenic embryos demonstrated increased H_2O_2 production in response to glucose exposure. This effect was completely blocked by the mitochondrial-specific H_2O_2/O_2^- quencher MitoQ (10μM) (n≥20/tx from 3 independent experiments).

Supplemental Figure 6 (related to Figure 6). Transcriptional analysis of glucose-treated embryos reveals changes in Hif1α signaling.

(A-D) Microarray analysis was conducted on RNA isolated from pooled cohorts of whole embryos exposed to 1% glucose from 12-36 hpf compared to untreated sibling controls (n=20).

(A) Ingenuity pathway analysis (IPA) revealed that the Top Canonical Pathway significantly regulated by glucose exposure is "Hif1α signaling", as determined by examination of all regulated genes (significant up- or down-regulation), as well as the cohort of genes with upregulated expression alone.

(B) IPA demonstrated "Hematological System and Function and Development", "Embryonic Development" and "Cardiovascular System Development and Function" were amongst the Top IPA Associated Network Functions based on total gene expression (up and down) influenced by glucose exposure.

(C) Hematological associated networks, such as "Immunological Disease", "Inflammatory Response", and "Hematological Disease" were amongst the Top IPA Biological Functions associated with glucose elevation based on the analysis of total up- and down-regulated genes, or those up-regulated alone following glucose exposure.

(D) Connectivity maps of glucose-regulated genes illustrate the node associated with Hif1α, as well as branches indicative of metabolism, proliferation, erythropoiesis and vasculogenesis.

Supplemental Figure 7 (related to Figure 7). Hif1α activity is required to mediate the effects of glucose metabolism on HSCs.

(A) *hif1a-like* expression, visualized in the tail region of the zebrafish embryo by *in situ* hybridization at 36hpf, was enhanced following glucose exposure from 12-36hpf (n≥25/tx).

(B) qPCR revealed upregulation of classical hif1α metabolic gene targets relevant to glucose transport and glycolysis after exposure to glucose (t-test, *$p<0.05$, n=3)

(C) Expression of the glucose transporter *glut1*, a classical transcriptional target of hif1α, was increased at 36hpf, following exposure to glucose (n≥25/tx).

(D) Quantitative analysis of fluorescence microscopy images of *cmyb:eGFP;lmo2:dsRed* reporter embryos revealed the positive effect of glucose exposure on HSCs could be abrogated by induction of dominant-negative (dn) *hif1a* (t-test, *$p<0.001$ vs control, **$p<0.001$ vs glucose, n=5).

(E) The increase in runx1+ cells caused by glucose in a *runx1:eGFP* reporter fish as detected by fluorescence microscopy at 36hpf was abolished by expression of *dnhif1a* (n≥20/tx).

(F) O-dianisidine staining at 36hpf revealed the enhancement in erythrocyte formation mediated by glucose was blocked after induction of *dnhif1a* (n≥25/tx).

(G) The effect of glucose exposure on *runx1/cmyb* expression in the AGM at 36hpf could not be fully abolished by MO-mediated knockdown of the hif1α target *vegfaa* (n≥45/tx).

S1A

D-Glucose

Control | 0.5% | 1% | 5%

runx1/cmyb

28/58 | 45/61 | 39/45

B

1% Glucose

Control | 12-36hpf | 12-24hpf | 24-36hpf

runx1/cmyb

n≥45/tx

fli1/flk1

n≥100/tx

36hpf

C

Control | D-Glucose

fli:GFP

34/35

D

qPCR Analysis

Relative Expression

2.5 | 2.0 | 1.5 | 1.0 | 0.5 | 0.0

flk1 | *tie2* | *lmo2* | *ve-cad*

E

sih+/+ or sih+/- | *sih-/-*

Control

Glucose

34/40

72/84

29/41

runx1/cmyb at 36hpf

F

Control | *sih*MO | Glucose | *sih*MO Glucose

Relative Expression

2.5 | 2.0 | 1.5 | 1.0 | 0.5 | 0.0

runx1 | *cmyb* | *CD41*

S2A

BrdU

Control

Glucose

22/31

B

In vivo Reporter

46/62

36hpf

C

AGM Region Cell Count

BrdU+ Cells/ Embryo [#]

30
20
10
0

*

Control

Glucose

D

Propidium Iodide FACS

Cell Count [%]

60
40
20
0

Control

Glucose

*

G1

S

G2

E

Hemocytometer Count

Total Cells/ Embryo [#]

20000
15000
10000
5000
0

NS

Control

Glucose

F

Bradford Assay

Protein [mg/fish]

0.15
0.10
0.05
0.00

NS

Control

Glucose

G

Control

Glucose

MHC

pax2

cmlc

foxA3

huc

n≥25/tx

36hpf

S3A

qPCR Time Course Analysis

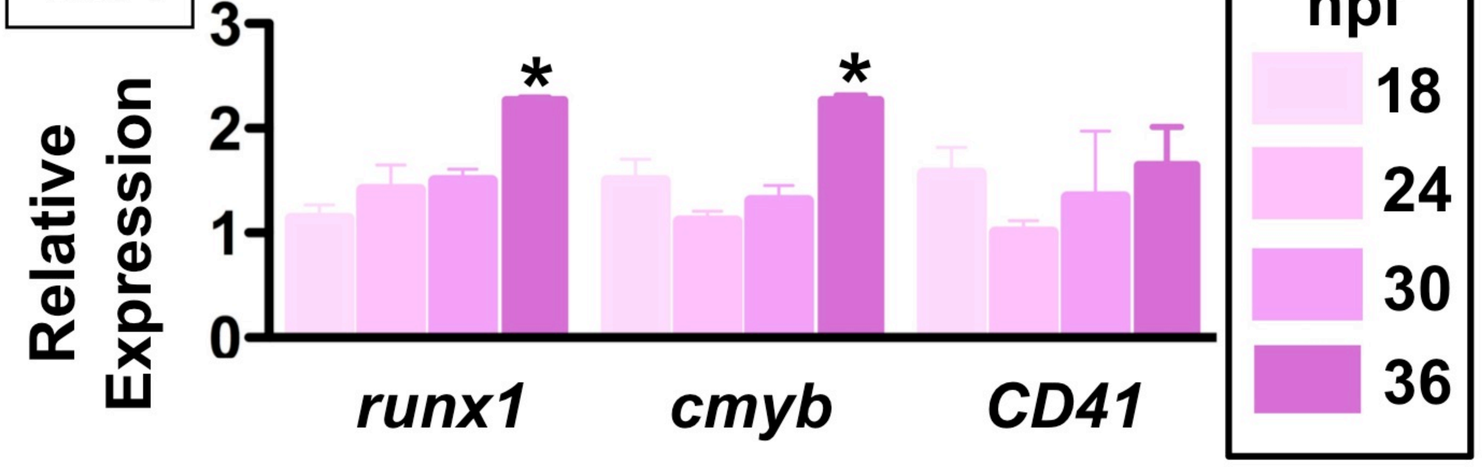

C

cmyb qPCR Analysis

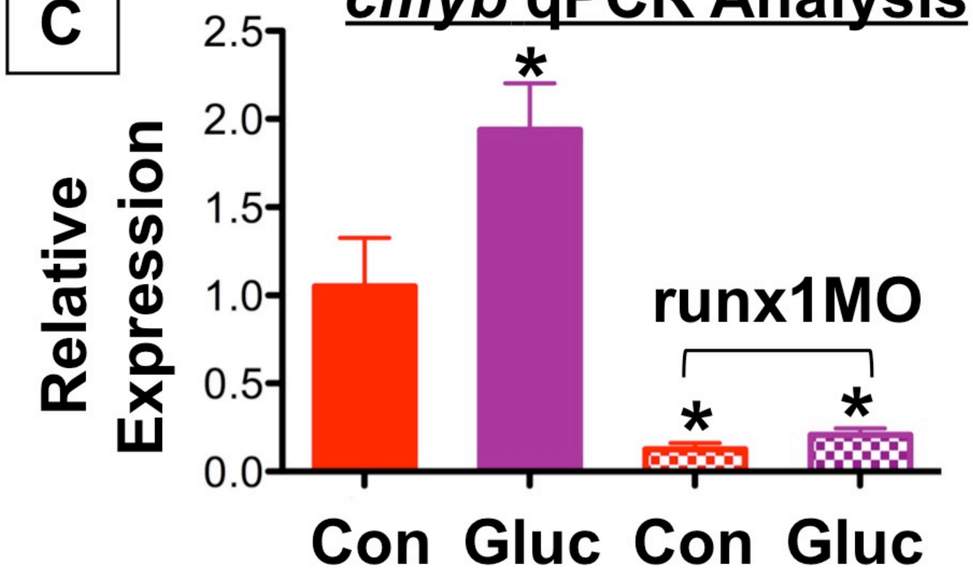

B

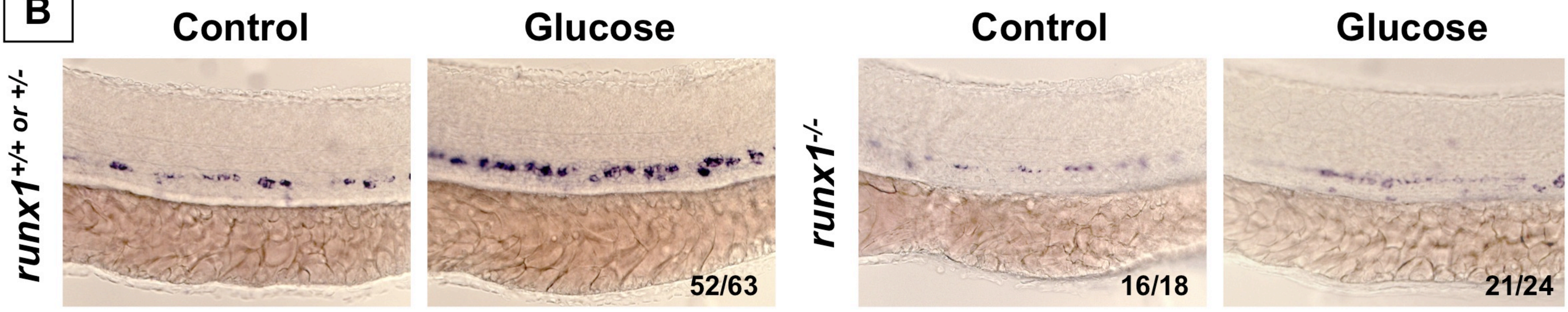

cmyb at 36hpf

D

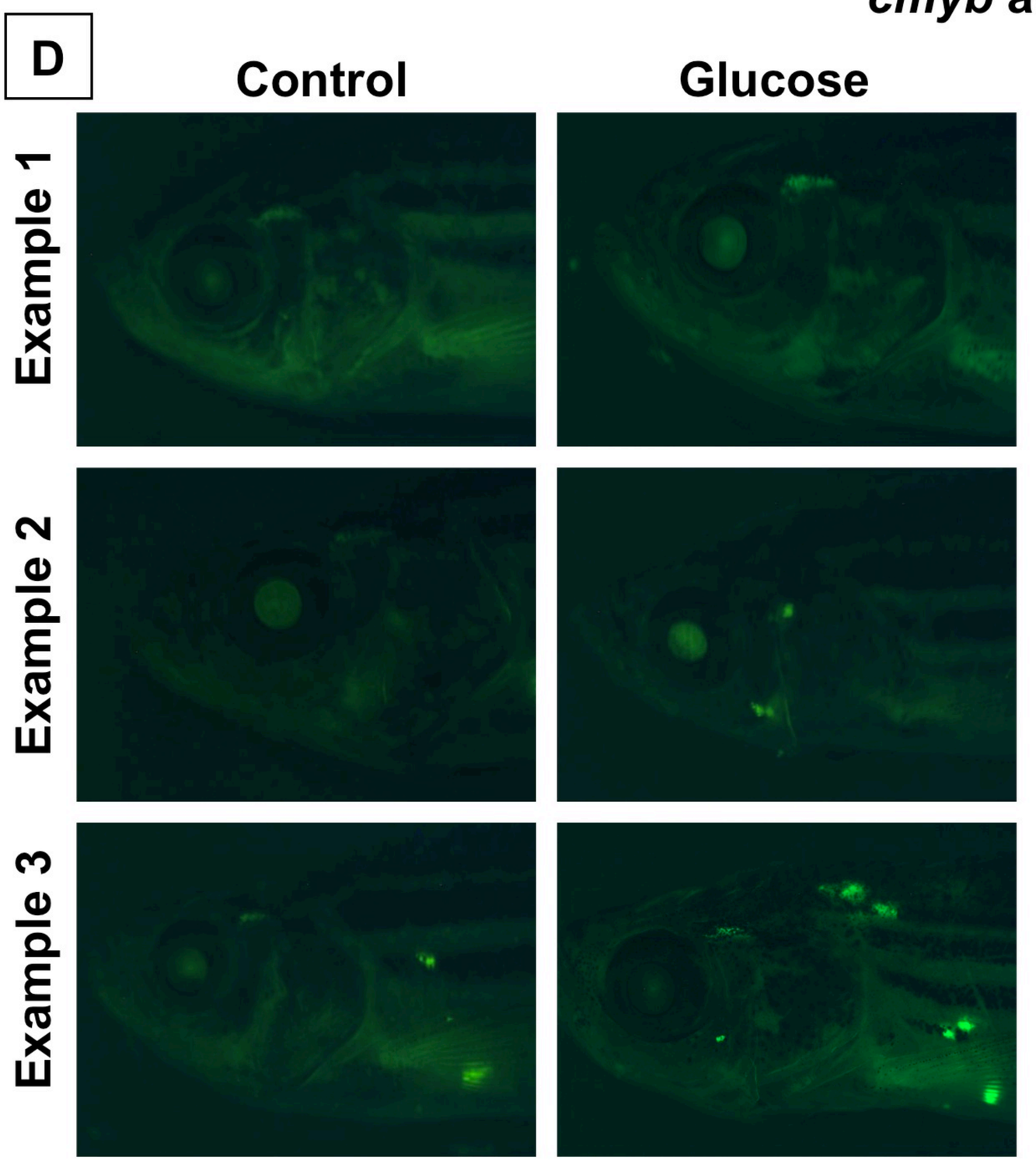

E

CD41:eGFP FACS Analysis

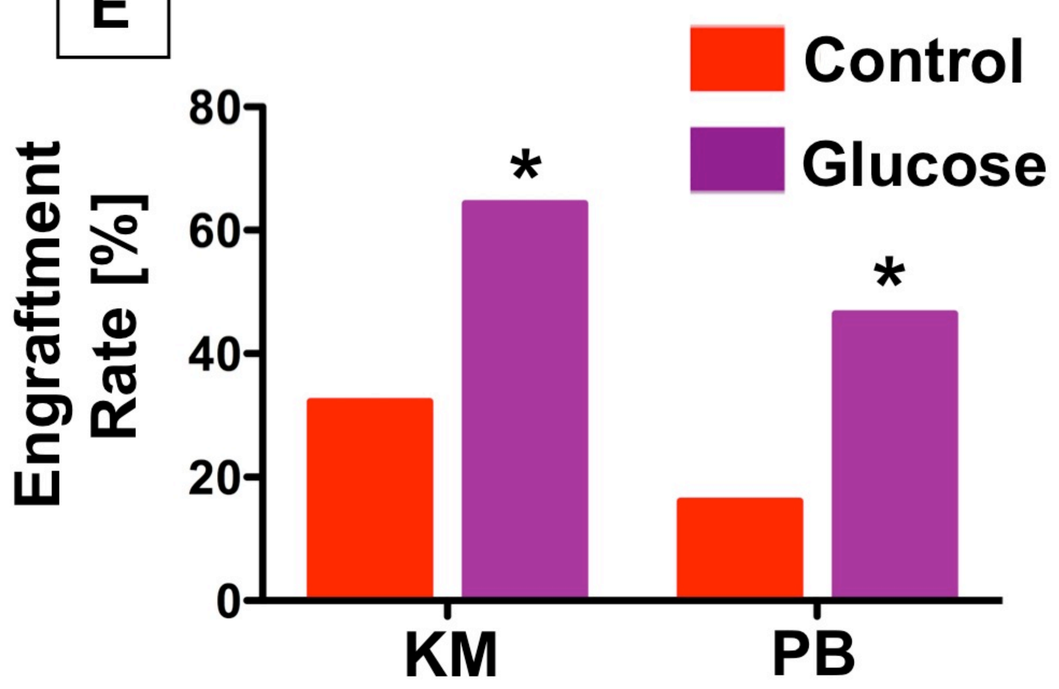

F

CD41:eGFP at 3wks post tx

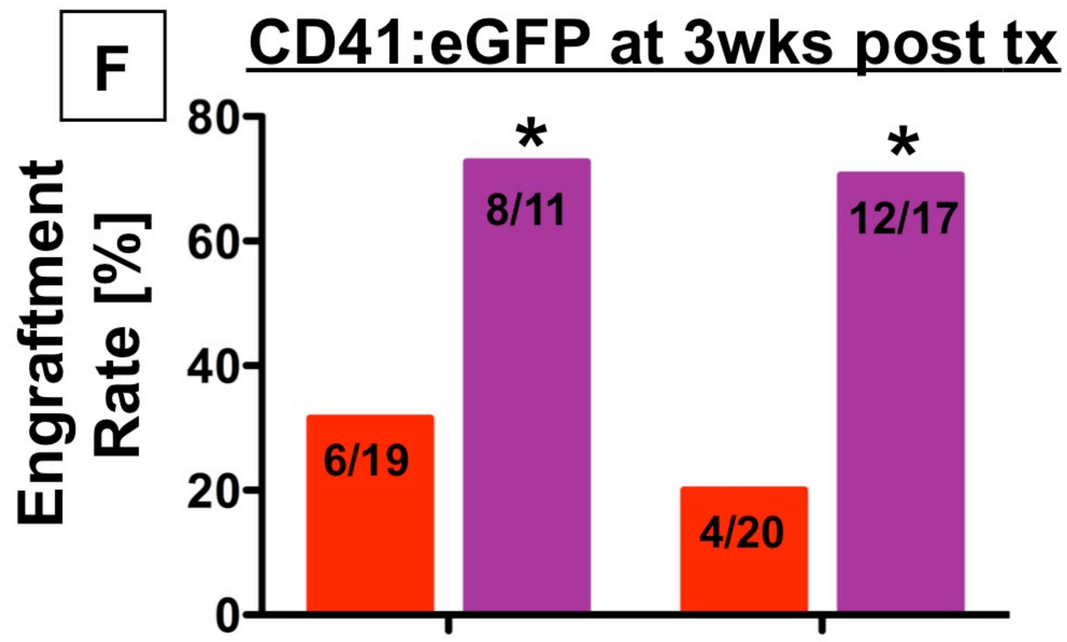

CD41:eGFP at 3wks post transplant

Replicate 1 Replicate 2

G

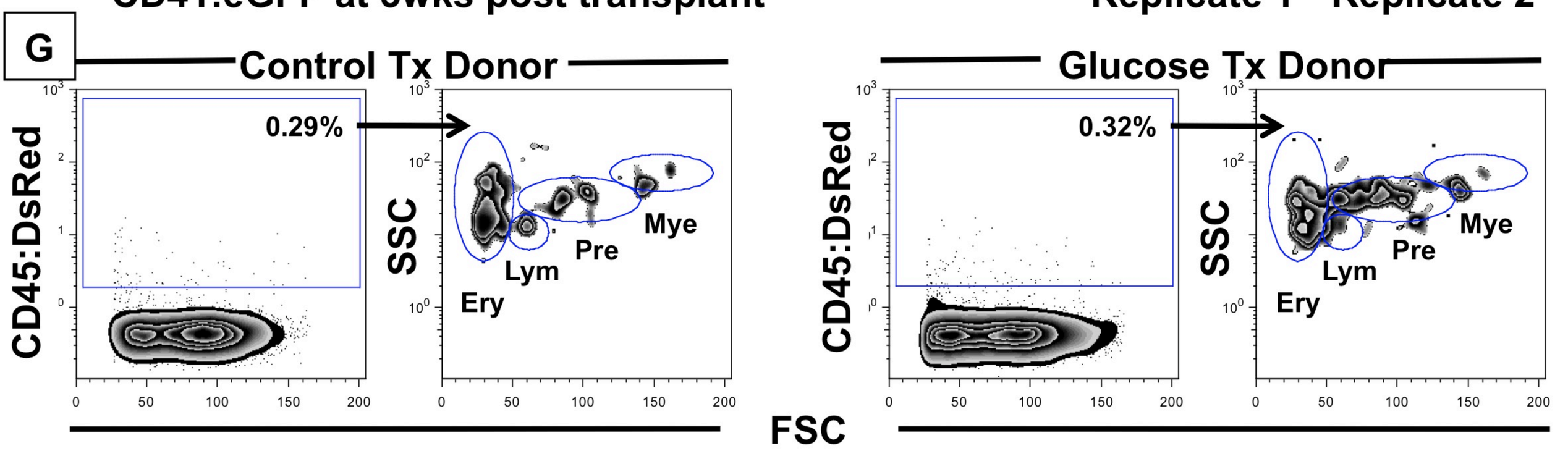

S4A

Control

Glucose

scl: eGFP

gata1: dsRed

globin: eGFP

26/42

30/35

33/38

B

FACS Analysis

Fluoro+ [% total]

scl gata1 globin

C

qPCR Analysis

Relative Expression

scl gata1 globin

Control

Glucose

D

CD41:eGFP

CHT

Kidney

48/53

31/37

E

FACS Analysis

5-36hr Tx

CD41:eGFP+ [% total]

Age [hours]

F

qPCR Analysis

5-36hr Tx

Relative Expression

lysc mpo rag2 lck

G

FACS Analysis

5-36hr Tx

Fluoro+ [% total]

lysc mpo rag2

H

Hemocytometer Ct

5-36hr Tx

Total Cell Number

Age [hours]

Control

Glucose

I

Absolute Number

5-36hr Tx

CD41 72 CD41 144 mpo 72 mpo 144 lysD 72 lysD 144

J

FACS Analysis

1 Month Post Tx

Frequency [% total]

Ery Lym Mye Pre HSC

K

FACS Analysis

Post 24hr Larval Tx

CD41:eGFP+ [% total]

Age [hours]

L

FACS Analysis

Day 10 Post injury

% Precursors

Control Glucose

S5A

Control

Glucose

Untreated

+ Streptozocin

Untreated

+ Streptozocin

n≥40/tx

insulin at 36hpf

B

DMSO

PTU

BSO

Paraquat

37/50

31/42

28/40

C

DMSO

Vitamin C

Euk134

MitoQ

Control

29/44

28/46

47/55

Glucose

29/35

30/45

17/30

40/52

runx1/cmyb at 36hpf

D

Control

Glucose

Untreated

+ MitoQ

Untreated

+ MitoQ

49/66

62/69

44/63

PeroxyFluor 2 H_20_2-reporter; *lmo2:dsRed* at 36hpf

S6A

Top Canonical Pathways	P=value
All Genes	
Hif1a Signaling	1.23E-03
Upregulated Genes	
Hif1a Signaling	2.45E-03

B

Associated Network Functions	Score
All Genes	
1. Drug Metabolism, Molecular Transport, Small Molecule Biochemistry	32
2. Hematological System Development and Function, Cellular Development, Hematopoiesis	24
3. Embryonic Development, Tissue Development, Cellular Assembly and Organization	22
4. Cardiovascular System Development and Function, Tissue Morphology, Organ Morphology	22
5. Behavior, Nervous System Development and Function, Infectious Disease	8
Upregulated Genes	
1. Lipid Metabolism, Molecular Transport, Small Molecule Biochemistry	33
2. Inflammatroy Response, Immunological Disease, Antigen Presentation	18
3. Cell Death, Hematological System Development and Function, Tissue Morphology	17
4. Cellular Compromise, Organ Development, Organ Morphology	3
5. Cell Cycle, DNA Replication, Recombination, and Repair, Embryonic Development	2

C

Top Bio Functions (Diseases and Disorders)	P=value
All Genes	
Immunological Disease	7.59E-05 - 1.11E-02
Developmental Disorder	1.20E-04 - 1.11E-02
Endocrine System Disorders	1.20E-04 - 1.11E-02
Infectious Disease	1.20E-04 - 2.20E-02
Inflammatory Disease	1.20E-04 - 1.31E-02
Upregulated Genes	
Immunological Disease	1.02E-03 - 4.56E-02
Hypersensitivity Response	1.32E-03 - 1.32E-03
Inflammatory Response	1.32E-03 - 3.56E-02
Cardiovascular Disease	1.60E-03 - 4.89E-02
Hematological Disease	2.27E-03 - 4.79E-02

D

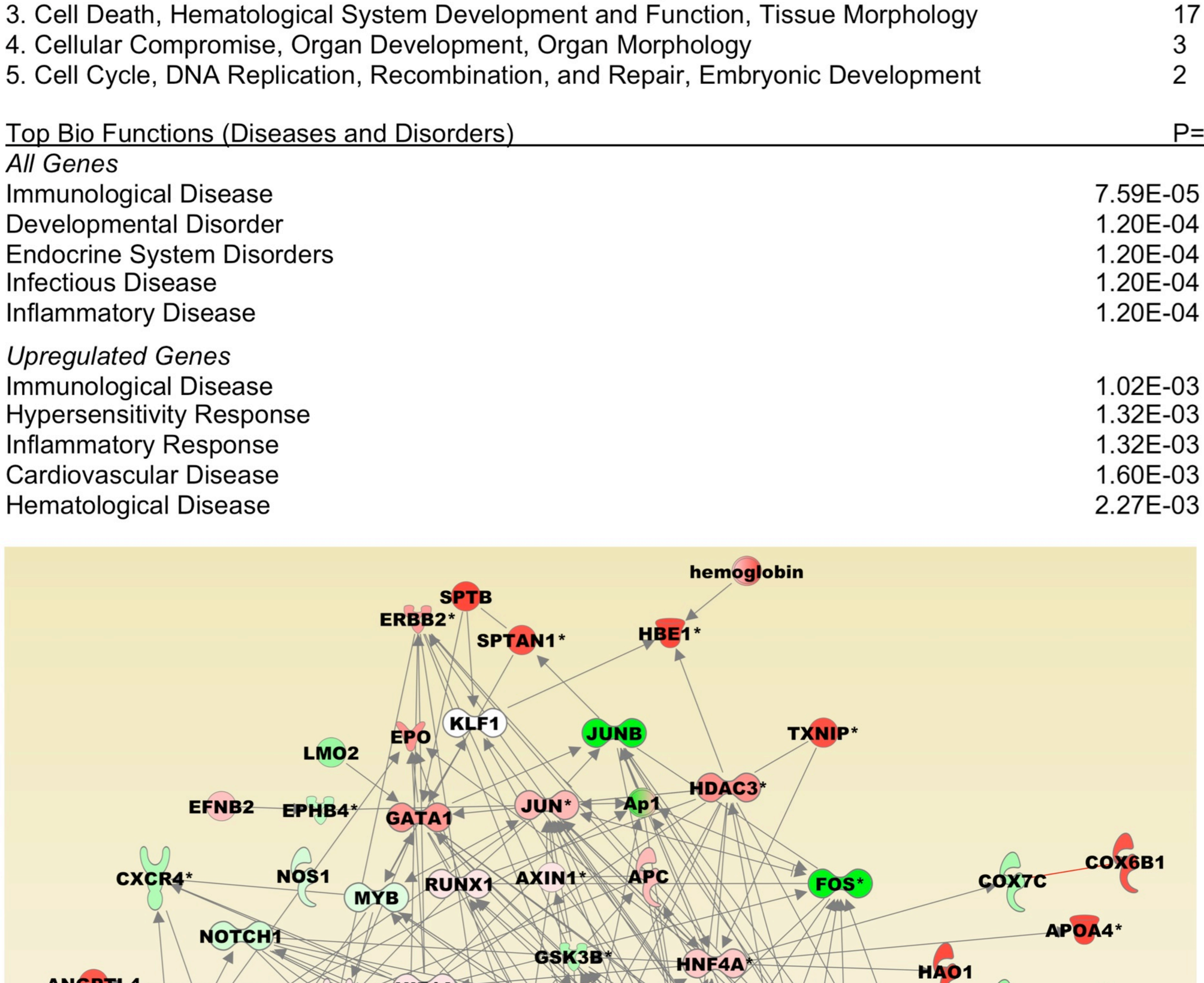

n≥20 embryos x 3 replicates/tx

S7A

Control

Glucose

View

side

AGM

22/25

hif1al at 36hpf

B

qPCR Analysis at 36hpf

Control

Glucose

Relative Expression

glut1 hk pfkl pklr pgk1 pdk2 g6pd ldha

C

Control

Glucose

View

side

top

18/21

glut1 at 36hpf

D

cmyb:GFP/lmo2:dsRed Microscopy

DP+ cells [#]

Control

Glucose

dnhif1a

dnhif1a + Glucose

E

Control

Glucose

Untreated

dnhif1a

19/23

25/30

18/25

runx1:eGFP at 36hpf

F

Control

Glucose

Untreated

dnhif1a

26/30

28/33

16/27

O-dianisidine at 36hpf

G

Uninjected

VEGFaa MO

Control

Glucose

40/52

52/58

29/47

runx1/cmyb at 36hpf

Supplemental Methods Table 1

Compound	Mechanism of Action	Concentration	Citation
lonidamine	hexokinase inhibitor	10 μM	(Floridi and Lehninger, 1983)
ethyl bromopyruvate	hexokinase II inhibitor	20 μM	(Ko et al., 2001)
potassium cyanide (KCN)	complex IV inhibitor	100 μM	(Nicholls et al., 1972)
oxaloacetic acid (OAA)	complex II inhibitor	50 μM	
N-Acetylcysteine (NAC)	antioxidant	10 μM	
MitoQ	antioxidant	10 μM	(Kelso et al., 2001)
Vitamin C	vitamin, antioxidant	750 μM	
Euk134	SOD mimetic	500 μM	(Rong et al., 1999)
propylthiouracil (PTU)	oxidant	0.003%	(Yu et al., 2010)
2,4-Dinitrochlorobenzene (DNCB)		0.5 μM	(Iijima et al., 2003)
L-buthionine sulphonximine (BSO)	GSH reductant	500 μM	(Griffith, 1982)
N,N'-dimethyl-4, 4'-biphyridinium dicholoride (Paraquat)	insecticide,	500 μM	(Bus and Gibson, 1984)
Colbalt Cloride ($CoCl_2$)	Hypoxia mimetic (directly binds hif1a to prevent breakdown)	500 μM	(Wang and Semenza, 1993)
Dimethyloxallyl Glycine (DMOG)	Competitive inhibitor of hif1a prolyl hydroxylase	50 μM	(Jaakkola et al., 2001)

References:

Bus, J.S., and Gibson, J.E. (1984). Paraquat: model for oxidant-initiated toxicity. Environ Health Perspect *55*, 37-46.

Floridi, A., and Lehninger, A.L. (1983). Action of the antitumor and antispermatogenic agent lonidamine on electron transport in Ehrlich ascites tumor mitochondria. Arch Biochem Biophys *226*, 73-83.

Griffith, O.W. (1982). Mechanism of action, metabolism, and toxicity of buthionine sulfoximine and its higher homologs, potent inhibitors of glutathione synthesis. J Biol Chem *257*, 13704-13712.

Iijima, N., Yanagawa, Y., and Onoe, K. (2003). Role of early- or late-phase activation of p38 mitogen-activated protein kinase induced by tumour necrosis factor-alpha or 2,4-dinitrochlorobenzene during maturation of murine dendritic cells. Immunology *110*, 322-328.

Jaakkola, P., Mole, D.R., Tian, Y.M., Wilson, M.I., Gielbert, J., Gaskell, S.J., Kriegsheim, A., Hebestreit, H.F., Mukherji, M., Schofield, C.J.*, et al.* (2001). Targeting of HIF-alpha to the von Hippel-Lindau ubiquitylation complex by O2-regulated prolyl hydroxylation. Science *292*, 468-472.

Kelso, G.F., Porteous, C.M., Coulter, C.V., Hughes, G., Porteous, W.K., Ledgerwood, E.C., Smith, R.A., and Murphy, M.P. (2001). Selective targeting of a redox-active ubiquinone to mitochondria within cells: antioxidant and antiapoptotic properties. J Biol Chem *276*, 4588-4596.

Ko, Y.H., Pedersen, P.L., and Geschwind, J.F. (2001). Glucose catabolism in the rabbit VX2 tumor model for liver cancer: characterization and targeting hexokinase. Cancer Lett *173*, 83-91.

Nicholls, P., van Buuren, K.J., and van Gelder, B.F. (1972). Biochemical and biophysical studies on cytochrome aa 3 . 8. Effect of cyanide on the catalytic activity. Biochim Biophys Acta *275*, 279-287.

Rong, Y., Doctrow, S.R., Tocco, G., and Baudry, M. (1999). EUK-134, a synthetic superoxide dismutase and catalase mimetic, prevents oxidative stress and attenuates kainate-induced neuropathology. Proc Natl Acad Sci U S A *96*, 9897-9902.

Wang, G.L., and Semenza, G.L. (1993). General involvement of hypoxia-inducible factor 1 in transcriptional response to hypoxia. Proc Natl Acad Sci U S A *90*, 4304-4308.

Yu, D., dos Santos, C.O., Zhao, G., Jiang, J., Amigo, J.D., Khandros, E., Dore, L.C., Yao, Y., D'Souza, J., Zhang, Z.*, et al.* (2010). miR-451 protects against erythroid oxidant stress by repressing 14-3-3zeta. Genes Dev *24*, 1620-1633.

Supplemental Methods Table 2

MO	Sequence	Reference
glut1 (slc2a1a)	GGCCATCATCAGCTGAGGAGTCACC	(Jensen et al., 2010)
insra	CGCGGTAAAGCCGAAAATCGTCCA	(Toyoshima et al., 2008)
insrb	CGCGACACGTTTTGGTTTCCTTGGA	(Toyoshima et al., 2008)
prdx1-ATG	AGCTGCCATTTTCTTGAACTGTCTT	not previously published
hif1ab	ACCCTACAAAAGAAAGAAGGAGAGC	(Mendelsohn et al., 2008)
vhl-ATG	GGCATCGTCAAAGACAGGACAGTTC	not previously published
vegfa	GTATCAAATAAACAACCAAGTTCAT	(Nasevicius et al., 2000)

Supplemental References:

Jensen, P.J., Gunter, L.B., and Carayannopoulos, M.O. (2010). Akt2 modulates glucose availability and downstream apoptotic pathways during development. J Biol Chem 285, 17673-17680.

Mendelsohn, B.A., Kassebaum, B.L., and Gitlin, J.D. (2008). The zebrafish embryo as a dynamic model of anoxia tolerance. Dev Dyn 237, 1780-1788.

Nasevicius, A., Larson, J., and Ekker, S.C. (2000). Distinct requirements for zebrafish angiogenesis revealed by a VEGF-A morphant. Yeast 17, 294-301.

Toyoshima, Y., Monson, C., Duan, C., Wu, Y., Gao, C., Yakar, S., Sadler, K.C., and LeRoith, D. (2008). The role of insulin receptor signaling in zebrafish embryogenesis. Endocrinology 149, 5996-6005.

Supplemental Methods Table 3

Gene	Forward	Reverse
b-actin	TCTGTCCCATGCCAACCAT	TGCCCTCGTGCTGTTTT
runx1	CGTCTTCACAAACCCTCCTCAA	GCTTTACTGCTTCATCCGGCT
cmyb	TGATGCTTCCCAACACAGAG	TTCAGAGGGAATCGTCTGCT
CD41	CTGAAGGCAGTAACGTCAAC	TCCTTCTTCTGACCACACAC
flk1	CGAACGTGAAGTGACATACGG	CCCTCTACCAAACCATGTGAAA
tie2	TGGAGGAGCGCAAGACATATG	CATTATTGCTGCAGTGCATCAG
lmo2	AAACACTGGAGGCAAATGAGGA	AGAAAGAAGCGGTCTCCGATG
ve-cad	ACACAAGATCCACACGCTGG	GAACATACACTCAGGAGCGTG
scl	CTCGAATGGTGCAGTTGAGTCC	GCATCTCCAGCAAAACCACTGT
gata1	TGAATGTGTGAATTGTGGTG	ATTGCGTCTCCATAGTGTTG
globin	TGGTTGTGTGGACAGACTTCGA	CGATAAGACACCTTGCCAGAGC
lysc	GTGAAAATGGACGGGCTGAA	CTTTGTTTGCGCTGCTCACA
mpo	TGATGTTTGGTTAGGAGGTG	GAGCTGTTTTCTGTTTGGTG
rag2	ACGCTCATGTCCAACTGGGATA	CTCTGCTGTCTACGCTCAACATGTA
lck	AGATGAATGGTGTGACCAGTGTA	GATCCTGTAGTGCTTGATGATGT
hk	CAACAACGCCACCGTCAAAATG	GCCCAGATCCAATGCCAAGAAA
pfkl	CGACAGGAACTTCGGCACTA	CCAATCACACATGCCGTATC
pklr	TAGAGGCCGTGGCCATGAT	GAGTCAAGCGCCGCAACT
pgk1	AGGAGGGCAAGGGCAAAG	CAGGGAGGCTCGGAAAGC
pdk2	CGAATTAGCCAATAAACCAACAAA	CACACTTCACCTGCATTTCCA
g6pd	GTCCCGAAAGGCTCCACTC	CCTCCGCTTTCCTCTC
ldha	GGCTATGGACTTGCAGCA	CTTTTGAGTTTGCGGTCAC
glut1	CCATTTCTCCTGGGCTTTACCTTTA	CAGATTTGGCTTTGCTTTCCTCGTT
phd3	AAAAACTGGAATGCCAAGGA	CGTAAGGTTTCCCTTCAGGA
epo	CGCGTCCTCGACCATTTC	TGCAATCGTCCTTACAAGTTCTCA
epoR	GTCAGATACGCTGTGGAGGA	TCACAGGACTGGTCCAAGAA
tfr	AATCGCATTATGAGGGTGGAA	GGGAGACACGTATGGAGAGAGC
tf	TTACATGGGAGGGTCCTAATGAG	GGACACAACTGCTCGAGAAGAA
vegf	CAGCTGTCAAGAGTGCCTACATAC	CATCAGGGTACTCCTGCTGAATTTC
flt	ATCATCTGGCTGAAGGATGG	AGGACACGCTCTTCTCTCCA
angpt1	CGCAGCCTCCTCAGCCTCTGTGCTA	CGATGTGGAAGCTGTCGTACTGA
angpt2	CACAGTGGCTGCAGAAGCTGGAGAG	CTGGAGTGGATATATCGTTACAG
ephrin	CCCACAAGAAATCCTCCAAA	ACTCTTCCCTCCGGATTCTC
tpo	ACCTGGCTGTGGACTCACTC	TTTGCCATCTCTGCAATGAG
nos1	CTCCATTCAGAGCCTTCTGG	CCGACAACCAAACACCAAG
nos2	GGGAAGACAAGCACAAACCAC	CGATGAAATCCTCTGCCTG
cxcr4	TGTACAGCAGCGTCCTCATC	ACCCAGGTGACAAACGAGTC
igf1	GTCTAGCGGTCATTTCTTCCA	ATCTGGCATCACACCTTCTACAAC
igf2	GAGTCCCATCCATTCTGTTG	TCCTTTGTTTGTTGCCATTTG
pdgfb	GGACCCTCTTCCTCCATCTC	TGGGACACGTAACTGACAGC
hif1a	CCATGAAGAGTTGAGAGAGATGCT	CTCTGTGTTTTGTTCCTTGGTCTTT
hif2a	ACGATAACTATCCCAGCTTTAACACA	CGACCGTGAGCGGGTTTA